

## Enhancement of coupled nitrification-denitrification by benthic photosynthesis in shallow estuarine sediments

Soonmo An

Marine Science Institute, University of Texas

Samantha B. Joye<sup>1</sup>

Department of Marine Sciences, University of Georgia

### Abstract

Net sediment-water interface fluxes of oxygen, dinitrogen, and dissolved inorganic carbon and nitrogen were determined in shallow, subtidal estuarine sediments (Galveston Bay, Texas) using in situ benthic chamber incubations. Diel variability in the sediment oxygen demand and in the flux of dinitrogen were attributable to the occurrence of benthic photosynthesis. Daytime denitrification rates exceeded nighttime rates. During daytime chamber incubations, small changes in dissolved oxygen concentration were observed. At night, oxygen concentrations decreased, as consumption reactions dominated the oxygen flux. Oxygen production by benthic microalgae enhanced rates of, and coupling between, nitrification and denitrification when ammonium was not limiting, resulting in significant loss of nitrogen from sediments as dinitrogen gas. A transient three box model was used to assess the effect of benthic primary production on sediment nitrogen cycling. Model results demonstrate increased rates of nitrification and denitrification in the presence of benthic photosynthesis and agree well with observed patterns of dissolved dinitrogen- and oxygen-flux data obtained during benthic chamber incubations. When no photosynthesis was permitted during the model runs, rates of nitrification and denitrification decreased significantly. Together, our results suggest that denitrification estimates for shallow estuaries could be underestimated if the influence of benthic primary production on denitrification is not considered.

Nitrification and denitrification are central processes in the sediment nitrogen (N) cycle. Nitrification represents the oxidation of ammonium ( $\text{NH}_4$ ) to nitrite ( $\text{NO}_2$ ) and, subsequently, nitrate ( $\text{NO}_3$ ), whereas denitrification represents reduction of  $\text{NO}_2$  or  $\text{NO}_3$  to gaseous forms, mainly nitrous oxide ( $\text{N}_2\text{O}$ ) or dinitrogen ( $\text{N}_2$ ). In sediments, these two processes may be coupled, with nitrifying bacteria providing the oxidized N source, which is subsequently consumed by denitrifying bacteria. The occurrence of coupled nitrification-denitrification, hereafter “coupled denitrification,” results in a net loss of bioavailable N from a system, since most organisms cannot assimilate  $\text{N}_2$  as an N source (Howarth et al. 1988). In contrast, organic N regenerated as dissolved inorganic N ([DIN] =  $\text{NH}_4 + \text{NO}_2 + \text{NO}_3$ ) can exert a strong influence on net system production, since primary production in marine systems is frequently N limited. High rates

of coupled nitrification-denitrification result in reduced rates of N regeneration, underscoring the need to understand the environmental and biogeochemical controls on nitrification and denitrification.

Both nitrification and denitrification are influenced by a variety of environmental parameters, including substrate availability, redox regime, the presence of inhibitors (e.g., sulfide,  $\text{S}^{2-}$ ), temperature, pH, and salinity (Henriksen and Kemp 1988; Seitzinger 1990; Joye and Hollibaugh 1995). Dissolved oxygen ( $\text{O}_2$ ) concentration impacts rates of nitrification and denitrification (Henriksen et al. 1981) because nitrifying bacteria are obligate aerobes, whereas denitrifying bacteria are facultative anaerobes (Tiedje et al. 1989). Therefore, processes that alter pore-water  $\text{O}_2$  concentration or the thickness of the oxic zone, such as benthic primary production, aerobic respiration, and aerobic oxidation of reduced metabolites, influence rates of these processes (Christensen et al. 1989; Nielsen et al. 1990; Rysgaard et al. 1995).

Photosynthesis can stimulate coupled denitrification by supplying  $\text{O}_2$  to nitrifiers, thereby stimulating nitrification and indirectly providing  $\text{NO}_3$  to denitrifiers. However, photosynthesis can inhibit denitrification by elevating the  $\text{O}_2$  concentration above a critical, inhibitory threshold ( $\sim 10 \mu\text{M}$ ; Tiedje et al. 1989), which results in a shift to aerobic respiration from denitrification (Koike and Sørensen 1988). The role of benthic photosynthesis as a stimulator ( $\text{O}_2$  supplier to nitrifiers) or inhibitor (DIN competitor with nitrifiers or  $\text{O}_2$  inhibition of denitrification) of coupled denitrification is influenced by water-column N inventories. For example, N limited phytoplankton may compete with nitrifiers for  $\text{NH}_4$ , whereas N-replete phytoplankton may not impact nitrifiers access to  $\text{NH}_4$ . Stimulation of coupled denitrification

<sup>1</sup> Corresponding author: (mjoye@arches.uga.edu)

### Acknowledgements

We thank L. Alford, S. Carini, R. Downer, S. Escorcía, R. Lee, K. Mace, A. Pichachy, and S. Ravula for assistance in the field and laboratory. Melanie Lesko, Susan Knock, and Ernest Estes at Texas A&M University's Pelican Island campus and Donald Harper, Charles Coleman, and Gary Gill at TAMU's Ft. Crockett campus arranged laboratory space and access to small boats and instrumentation. D. Brock, P. Eldridge, and J. Pinckney provided stimulating discussions about the Galveston Bay ecosystem; and C. Meile, W. Gardner, and two anonymous referees provided valuable comments that improved this manuscript.

This work was supported by the National Science Foundation (grants OCE 96-96054 and 98-96216) and the Texas Water Development Board (grants 96-167, 97-218, and 98-239).

by benthic photosynthesis in lake and estuarine sediments has been reported under N-replete conditions (Risgaard-Petersen et al. 1994; Rysgaard et al. 1995; Tomaszek et al. 1997). Inhibition of nitrification and denitrification, due to competition between microalgae and nitrifiers and denitrifiers for DIN, has been inferred when pore-water and/or bottom-water DIN concentration is low (Nielsen et al. 1990; Nielsen and Sloth 1994).

Benthic primary production requires that sufficient light energy (i.e., photosynthetically active radiation [PAR]) reach the sediment-water interface. However, PAR may limit nitrification, particularly the process of  $\text{NO}_2$  oxidation. Field data suggest, however, that nitrification occurs within the euphotic zone of many aquatic systems (Ward et al. 1989; Joye et al. 1999). Studies of nitrifying bacteria in culture have shown that both  $\text{NH}_3$  and  $\text{NO}_2$  oxidizers are sometimes sensitive to near UV (300–375 nm) and blue-spectrum (400–475 nm) light. However, sensitivity depends on the type of nitrifier and the absorbance properties of the media (Guero and Jones 1996a,b).

Galveston Bay is a shallow, microtidal estuary along the Texas coast. Current estimates of denitrification in Galveston Bay range between 0.4 (Zimmerman and Benner 1994) and  $10 \text{ mmol m}^{-2} \text{ d}^{-1}$  (G. Rowe pers. comm.). Modeling of available denitrification-rate data suggests that denitrification removes between 7% and 66% of the annual baywide N load. The large range of available denitrification data raises questions regarding the importance of denitrification in the N budget of Galveston Bay. In previous studies, denitrification rates were not directly quantified (as  $\text{N}_2$  gas) in situ, and only Zimmerman and Benner (1994) examined rates over an annual cycle at the same stations.

By measuring denitrification rates directly at the same stations over annual cycles between 1996 and 1998, we obtained improved estimates of denitrification for the Galveston Bay system and reevaluated the system N budget. During January and August of 1997, we performed diel studies of benthic metabolism and denitrification during clear benthic chamber incubations over 24–48 h. In addition to quantifying sediment-water exchange of dissolved gases (dissolved inorganic carbon [DIC],  $\text{O}_2$ , and  $\text{N}_2$ ), we determined fluxes of DIN, benthic chlorophyll *a* concentration, and pore-water profiles of dissolved nutrients. Our overall objective was to quantify denitrification rates, assess daily patterns of activity, and elucidate the environmental factors driving these patterns. Here, we report rates of denitrification determined directly in benthic chambers and use a transient three-box model to evaluate linkages between benthic primary production and N cycling.

## Methods

*Study site*—The Galveston Bay estuarine ecosystem is the second largest estuary on the Texas coast. The Houston metropolitan area surrounds the bay, and 3.5 million people inhabit the watershed. The primary site discussed in this paper lies in central Galveston Bay (Texas City:  $94^\circ 49' 65'' \text{W}$ ,  $29^\circ 23' 51'' \text{N}$ ). The water depth is  $\sim 4$  m, and the sediment is composed of sands ( $< 1.0\%$  organic carbon,  $95\% > 63 \mu\text{m}$ ).

Water-column temperature and salinity were low ( $14^\circ\text{C}$ , 1–5 ppt) during winter and increased during summer ( $28^\circ\text{C}$ – $32^\circ\text{C}$ , 25–32 ppt). Water-column dissolved  $\text{O}_2$  concentration exhibited a surface to bottom decrease of  $1\text{--}2 \text{ mg L}^{-1}$ ; however, bottom-water  $\text{O}_2$  concentration always exceeded  $5 \text{ mg L}^{-1}$ . Bottom-water nutrient concentrations were high in winter (DIN  $\sim 23 \mu\text{M}$ ,  $\text{PO}_4 \sim 1 \mu\text{M}$ ) and low in summer (DIN  $\sim 1.6 \mu\text{M}$ ,  $\text{PO}_4 \sim 0.3 \mu\text{M}$ ). Similarly, pore-water nutrient concentrations in the upper 5 cm were low during winter (DIN  $< 50 \mu\text{M}$ ,  $\text{PO}_4$  below detection) but increased during summer (DIN  $\sim 130 \mu\text{M}$ ,  $\text{PO}_4 \sim 10 \mu\text{M}$ ). Benthic Chl *a* concentration in the upper 0.5 cm varied between 250 and  $800 \text{ mg Chl } a \text{ m}^{-2}$  over the annual cycle. Estimates of PAR reaching the sediments were obtained from secchi depth data.

*Field methods*—In situ sediment-water fluxes of DIC,  $\text{N}_2$ ,  $\text{O}_2$ , and DIN were determined in clear acrylic benthic chambers ( $900 \text{ cm}^2$  area and 9 L volume;  $n = 2\text{--}4$  per site), which were placed onto the sediment by SCUBA divers. Chamber water samples were collected at set time points during diel experiments (after 0, 11, 22, and 35 h in August and 0, 19, and 35 h in January). Triplicate samples from each chamber for  $\text{O}_2$  and  $\text{N}_2$  analyses were collected into 10-ml gas-tight glass syringes, which were closed using three-way stopcocks and stored at  $5^\circ\text{C}$  until analysis via gas chromatography (An and Joye 1997). Laboratory experiments illustrated that syringes could be stored for up to 14 d without significant change in gas concentrations. Duplicate samples for DIC concentration determination were transferred from 100-ml syringes into 10-ml glass vials without introducing bubbles, preserved by adding  $200 \mu\text{l}$  of saturated  $\text{HgCl}_2$  solution and then sealed with a Teflon-lined cap. DIC concentration was quantified via coulometric titration within 4 weeks. The remaining sample in the 100-ml syringe was passed through a GF/F filter and collected into a 10% acid-cleaned, milli-Q water-rinsed plastic bottle and frozen for subsequent analysis of nutrient concentrations.

Sediment cores (40-cm depth) were collected by SCUBA divers and maintained at field temperatures in the dark for 3–6 h during transport back to the laboratory and processing. Cores were sectioned at centimeter-scale intervals and pore water was extracted under an  $\text{N}_2$  atmosphere using a Reeber squeeze. Expressed pore water was collected into a syringe and then passed through a GF/F filter into a clean 10-ml glass vial and stored frozen prior to analysis. For chamber and pore-water samples, nitrite + nitrate (denoted  $\text{NO}_3$ ) concentration was determined by use of standard methods on an Alpkem FlowSolution 3000 Autoanalyzer. Ammonium concentrations were determined colorimetrically by use of the phenol hypochlorite method (Soloranzo 1969; Koroleff and Grasshoff 1983). Chl *a* was extracted in 100% acetone, and pigment concentration was determined by use of spectrophotometric methods (Pinckney et al. 1994).

*Model background, assumptions, and limitations*—A transient three box model was developed to evaluate the effect of benthic photosynthesis on coupled denitrification. Flux measurements during winter (January) and summer (August) of 1997 were compared with model results, to elucidate the

Table 1. Content and physical-biological processes in each Box described by the transient model.

Box content	Box 1 Bottom water inside the chamber	Box 2 Oxic-suboxic surface sediment	Box 3 Anoxic sediment
Height (cm)	10	1	9
Processes permitted	Diffusion	Diffusion Aerobic respiration Reoxidation of reduced material Photosynthesis Nitrification Denitrification	Diffusion Aerobic respiration Anaerobic respiration  Nitrification Denitrification

processes responsible for the observed concentration changes in each box. Diagenetic models describing organic matter degradation and relevant environmental processes are available. Although such models are valuable tools for elucidating many early diagenetic processes (Middelburg et al. 1996; Wang and Van Cappellen 1996; Boudreau 1997), they are not currently appropriate for the description of the hourly to daily changes observed during our work. Our transient model permitted us to compare rates of denitrification with and without benthic primary production. This model required fewer assumptions, thus simplifying the task of identifying the mechanisms driving observed concentration changes.

**Model description**—The transient model describes the temporal evolution of dissolved O<sub>2</sub>, N<sub>2</sub>, and DIN concentration in three boxes that comprised the benthic incubation chamber system. Important biogeochemical processes were described in the water overlying the sediment (Box 1), in oxic-suboxic surface sediment (Box 2) and in anoxic sediment (Box 3; Table 1). The major processes controlling the concentration of O<sub>2</sub>, N<sub>2</sub>, and DIN in the overlying water and sediment pore water includes diffusion, organic matter degradation, photosynthesis, nitrification, and denitrification

(Table 1). In coastal environments, water column bacterial density is small (10<sup>6</sup> cells ml<sup>-1</sup>), compared with sediment bacterial density (~10<sup>9</sup>–10<sup>10</sup> cells ml<sup>-1</sup> (Ducklow 1983). Similarly, the Chl *a* concentration in the overlying water column of our benthic chambers (0.01–0.1 mg Chl *a* m<sup>-2</sup>) is much less than the sediment Chl *a* concentration (9–45 mg Chl *a* m<sup>-2</sup>). Water-column respiration rates were insignificant (i.e., there was no significant change in O<sub>2</sub> concentration over a 24-h incubation period; initial [O<sub>2</sub>] = 175.0 ± 0.4 μM and final [O<sub>2</sub>] = 174.5 ± 0.3 μM; S. An unpubl. data). Together, these data led us to conclude that water-column processes in the chambers were insignificant when compared with sediment processes.

In Box 1, only diffusive exchange with surface sediment was permitted to alter the concentration of a constituent. In Box 2, organic matter degradation was mediated by aerobic (O<sub>2</sub> respiration) or suboxic (denitrification) processes, and oxidation of reduced compounds was also permitted (Table 2). In Box 3, anaerobic (≈sulfate reduction) processes, as well as aerobic oxidation reactions, were permitted. However, aerobic processes in Box 3 were insignificant, since they were limited by O<sub>2</sub> availability in the anoxic sediment. Transport between Box 2 and between Boxes 1 and 3 was

Table 2. Parameters used in the transient model for summer and winter simulations.

Parameter	Symbol	Summer	Winter	Units	Reference
Temperature	C	30	15	°C	
Diffusion distance between boxes	X <sub>i</sub>	0.1	0.35	cm	See text
Diffusion coefficient	DO <sub>2</sub>	9.2	8.7	10 <sup>-6</sup> cm <sup>2</sup> s <sup>-1</sup>	Boudreau (1997)
	DN <sub>2</sub>	8.2	7.7	10 <sup>-6</sup> cm <sup>2</sup> s <sup>-1</sup>	Boudreau (1997)
	DNO <sub>3</sub>	8.5	6.2	10 <sup>-6</sup> cm <sup>2</sup> s <sup>-1</sup>	Boudreau (1997)
	DNH <sub>4</sub>	8.8	6.4	10 <sup>-6</sup> cm <sup>2</sup> s <sup>-1</sup>	Boudreau (1997)
Maximum aerobic respiration rate*	R <sub>o</sub>	100	15	mmol m <sup>-2</sup> d <sup>-1</sup>	See text
Anaerobic respiration rate†	AR	11	7	mmol m <sup>-2</sup> d <sup>-1</sup>	See text
Maximum denitrification rate*	DN <sub>max</sub>	75	45	mmol m <sup>-2</sup> d <sup>-1</sup>	See text
Photosynthesis rate*	P <sub>max</sub>	105	37	mmol m <sup>-2</sup> d <sup>-1</sup>	See text
Nitrification rate constant	K <sub>NH<sub>4</sub>OX</sub>	60	30	10 <sup>-6</sup> μM <sup>-1</sup> s <sup>-1</sup>	Van Cappellen and Wang (1996)
Half saturation constant for O <sub>2</sub> during aerobic respiration	K <sub>O<sub>2</sub></sub>	8	8	μM	Boudreau (1996)
Half saturation constant for NO <sub>3</sub> during denitrification	K <sub>NO<sub>3</sub></sub>	30	30	μM	Boudreau (1996)
Inhibition constant for O <sub>2</sub> during denitrification	K' <sub>O<sub>2</sub></sub>	8	8	μM	Boudreau (1996)

\* Gross rate.

† Net rate.

described by diffusion. Anaerobic processes mediate a substantial portion of organic matter degradation in coastal sediments (Capone and Kiene 1988), and a constant rate of anaerobic respiration ( $R_A$ ) was used for Box 3. Anaerobic respiration rates often exceed aerobic respiration rates in coastal environments (Jørgensen 1977; Howes et al. 1984); however, the permeable sands at this site could support high rates of aerobic respiration (Sørensen et al. 1979; Capone and Kiene 1988). Results of an inverse model analysis suggest that sulfate reduction accounted for 30% of organic matter oxidation, whereas aerobic respiration accounted for 25% of organic matter oxidation (An 1999). In the current model, sulfate reduction rates estimated from this inverse analyses were used to represent anaerobic process (7 and 11 mmol  $m^{-2} d^{-1}$  in winter and summer, respectively; Table 2; An 1999). These values are similar to documented sulfate reduction rates in Galveston Bay (J. W. Morse unpubl. data).

Apparent diffusion coefficients for gases and ions were used to calculate infinite dilution diffusion coefficients, using regressions against temperature and modified to account for salinity and tortuosity under the assumption of a constant porosity (0.8) (Boudreau 1997; Table 2). The flux between adjacent boxes was modeled by use of Fick's First Law of Diffusion:

$$f_i = D_x \frac{\Delta C_i}{X_i}, \quad (1)$$

where  $f_i$  is the flux from Box  $i$  to Box  $i + 1$ ,  $D_x$  is the diffusion coefficient of species  $x$ ,  $\Delta C_i$  is the concentration difference between Box  $i$  and Box  $i + 1$  of a chemical species, and  $X_i$  is the thickness of the diffusion layer—i.e., the average distance between Box  $i$  and Box  $i + 1$  that a chemical species has to travel to contribute to the concentration of the other Box. The rate of  $O_2$  concentration change in Box 1 depends on  $O_2$  consumption rates in Boxes 2 and 3 and on the diffusion distance. The diffusion distance was adjusted to replicate the measured sediment oxygen demand and was considered constant for all chemical species (Table 2).

Rates of specific processes were modeled as follows. Aerobic organic matter degradation was described by use of Monod kinetics (Boudreau 1997). Gross maximum rates of aerobic respiration ( $R_o$ ) used for winter and summer (Table 2) lie within the range observed in other coastal environments (Jørgensen 1977; Howarth and Teal 1979). Nitrification (N) depends on the availability of  $NH_4$  and  $O_2$  (Henriksen and Kemp 1988), so rates were modeled as the product of a rate constant and the  $O_2$  and  $NH_4$  concentration (Table 2; Boudreau 1997). Denitrification (DN) was modeled using Monod kinetics including an inhibition term for  $O_2$  (Table 2; Boudreau 1997). Maximum rates of denitrification ( $DN_{max}$ ) were obtained by varying  $DN_{max}$  so as to replicate observed  $N_2$  fluxes; this term differed in summer and winter. Daily variations in PAR could drive diel variation in benthic primary production. However, to simplify the modeling effort, a constant photosynthetic rate ( $P_{max}$ ) was used during the day, and no photosynthesis was permitted at night (Table 2). The value of  $P_{max}$  was set so as to reproduce the changes in  $O_2$  and  $N_2$  concentration observed during chamber incubations.

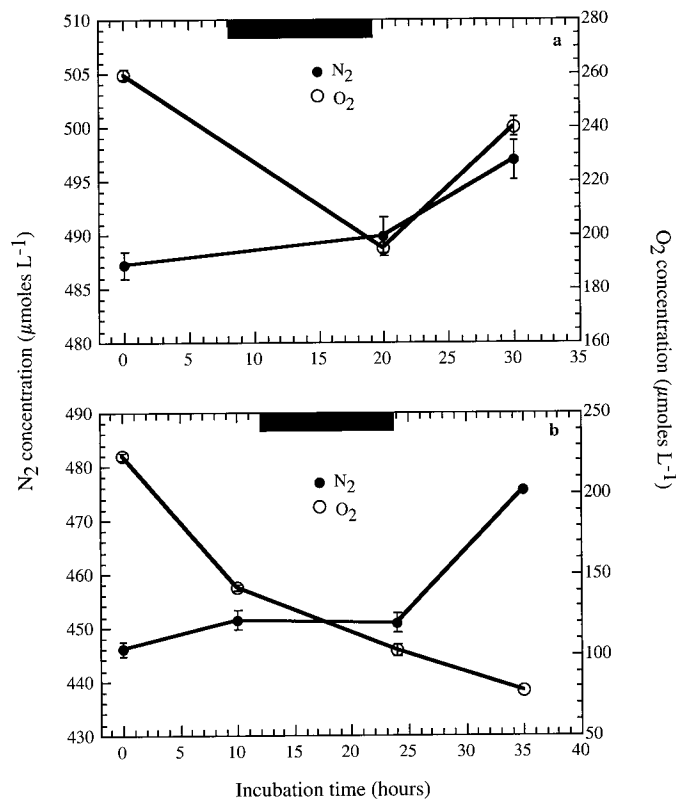


Fig. 1. Concentration changes of  $N_2$  and  $O_2$  during in situ chamber incubations at the Texas City station in (a) January 1997 and (b) August 1997. Each symbol represents the average (error bars are the standard deviation of the mean) from three incubation chambers (triplicate samples from each chamber at each time point). The filled bar on the top x axis represents the dark portion of the incubation.

*Parameter adjustment and solving the equations*—Model constants were selected by varying values until the observed concentration changes in Box 1 were reproduced (Fig. 1; Table 2). Concentration changes with time in each Box were described with use of differential equations (Table 3). Sensitivity to constant values was evaluated by halving or doubling the value (Table 4). Equations were solved by use of an ordinary differential equation solver (ode45) in Matlab. The initial values of  $NH_4$  and  $NO_3$  in Boxes 2 and 3 were obtained from pore-water data. Time zero concentrations were used for the initial values of  $O_2$ ,  $N_2$ , and DIN (when chamber and bottom-water concentrations were equivalent).

## Results and discussion

*Field results*—Diel patterns of  $O_2$  and  $N_2$  flux were observed in Texas City sediments, suggesting a daytime enhancement of denitrification by benthic primary production. Benthic primary production is not unique to this location in Galveston Bay. We observed net  $O_2$  production during chamber incubations at a variety of Bay locations, as did Warnken (1998). In winter (January), the  $O_2$  concentration increased during the daytime-only incubation and decreased at night (Fig. 1; Table 5). Denitrification rates, evidenced by in-

Table 3. Equations describing the concentration changes of oxygen (O), nitrate (NN), ammonium (AM), and nitrogen gas (N<sub>2</sub>) in the three box model. Subscript denotes Box number. The variables are:  $h_i$ , height of Box  $i$ ;  $X_i$ , diffusion distance;  $\phi$ , porosity (0.8);  $\alpha$ , organic carbon to nitrogen ratio of reacting organic matter (6.6);  $D_s$ , diffusion coefficient of given chemical species  $s$ ;  $P$ , photosynthesis;  $U$ , proportion of NH<sub>4</sub> used as the N source during benthic photosynthesis (0.9; Falkowski and Raven 1997);  $R_{O_2}$ , aerobic respiration;  $R_A$ , anaerobic respiration;  $N_i$ , nitrification; and  $DN_i$ , denitrification. Values of constants are presented in Table 2. Equations 1, 5, and 9 describe the change in O<sub>2</sub> concentration over time in Boxes 1, 2, and 3, respectively. Equations 2, 6, and 10 describe the change in NO<sub>2</sub> + NO<sub>3</sub> concentration over time in Boxes 1, 2, and 3, respectively. Equations 3, 7, and 11 describe the change in NH<sub>4</sub> concentration over time in Boxes 1, 2, and 3, respectively. Equations 4, 8, and 12 describe the change in N<sub>2</sub> concentration over time in Boxes 1, 2, and 3, respectively. Equations 13, 14, and 15 present the Monod formulations for calculating rates of aerobic respiration (13), nitrification (14), and denitrification (15).

---



---

Box 1:

---

$$\frac{d[O]_1}{dt} = \frac{D_{O_2}}{h_1} \left( \frac{[O]_1 - [O]_2}{X_1} \right), \quad (1)$$

$$\frac{d[NN]_1}{dt} = \frac{D_{NO_2}}{h_1} \left( \frac{[NN]_1 - [NN]_2}{X_1} \right), \quad (2)$$

$$\frac{d[AM]_1}{dt} = \frac{D_{NH_4}}{h_1} \left( \frac{[AM]_1 - [AM]_2}{X_1} \right), \quad (3)$$

$$\frac{d[N_2]_1}{dt} = \frac{D_{N_2}}{h_1} \left( \frac{[N_2]_1 - [N_2]_2}{X_1} \right). \quad (4)$$


---

Box 2:

---

$$\frac{d[O]_2}{dt} = \frac{1}{h_2\phi} \left[ P - R_{O_2} - D_{O_2} \left( \frac{[O]_1 - [O]_2}{X_1} \right) + D_{O_2} \left( \frac{[O]_3 - [O]_2}{X_2} \right) - R_A \right] - 2N_2, \quad (5)$$

$$\frac{d[NN]_2}{dt} = \frac{1}{h_2\phi} \left[ -DN_2 - (1 - U)\alpha p - D_{NO_3} \left( \frac{[NN]_1 - [NN]_2}{X_1} \right) + D_{NO_3} \left( \frac{[NN]_3 - [NN]_2}{X_2} \right) \right] + N_2, \quad (6)$$

$$\frac{d[AM]_2}{dt} = \frac{1}{h_2\phi} \left[ \alpha R_{O_2} - U\alpha p - D_{NH_4} \left( \frac{[AM]_1 - [AM]_2}{X_1} \right) + D_{NH_4} \left( \frac{[AM]_3 - [AM]_2}{X_2} \right) \right] - N_2, \quad (7)$$

$$\frac{d[N_2]_2}{dt} = \frac{1}{h_2\phi} \left[ \frac{DN_2}{2} - D_{N_2} \left( \frac{[N_2]_1 - [N_2]_2}{X_1} \right) + D_{N_2} \left( \frac{[N_2]_3 - [N_2]_2}{X_2} \right) \right]. \quad (8)$$


---

Box 3:

---

$$\frac{d[O]_3}{dt} = \frac{1}{h_3\phi} \left[ -R_{O_3} - D_{O_2} \left( \frac{[O]_3 - [O]_2}{X_2} \right) \right] - 2N_3, \quad (9)$$

$$\frac{d[NN]_3}{dt} = \frac{1}{h_3\phi} \left[ -DN_3 - D_{NO_3} \left( \frac{[NN]_3 - [NN]_2}{X_2} \right) \right] + N_3, \quad (10)$$

$$\frac{d[AM]_3}{dt} = \frac{1}{h_3\phi} \left[ \alpha R_{O_3} + R_A - D_{NH_4} \left( \frac{[AM]_3 - [AM]_2}{X_2} \right) \right] - N_3, \quad (11)$$

$$\frac{d[N_2]_3}{dt} = \frac{1}{h_3\phi} \left[ \frac{DN_3}{2} - D_{N_2} \left( \frac{[N_2]_3 - [N_2]_2}{X_2} \right) \right], \quad (12)$$

where

$$R_{O_i} = R_{O_{\max}} \frac{[O]_i}{(K_{O_X} + [O]_i)}, \quad (13)$$

$$N_i = K_{NH_4OX} [O]_i [AM]_i, \quad (14)$$

$$DN_i = DN_{\max} \frac{[NN]_i}{(K_{NO_3} + [NN]_i)} \frac{K'_{O_2}}{(K'_{O_2} + [O]_i)}. \quad (15)$$


---

Table 4. Comparison between observed sediment oxygen demand (SOD) and dinitrogen ( $N_2$  flux) and model results as a function of varying diffusion distance  $X_i$ , maximum respiration ( $R$ ), and photosynthetic rates ( $P$ ). The complete model contains the values used in the general model scheme. The terms  $X_i$ ,  $R$ , and  $P$  were halved or doubled from complete model values to evaluate the effect on fluxes. All units are  $mmol\ m^{-2}\ d^{-1}$  except  $X_i$  (cm).

Field data:	Winter										Summer									
	Model variation:	$X_i$	$R_{max}$	$P$	SOD		$N_2$ flux		$X_i$	$R_{max}$	$P$	SOD		$N_2$ flux						
					Light	Dark	Light	Dark				Light	Dark	Light	Dark					
Rate observed in chambers:					10.30	-7.40	1.00	0.48				-7.5	-11.2	2.2	0.1					
Model results:																				
Model variation:	Complete	0.35	15	37	-1.00	-4.70	0.90	0.38	0.10	100	105	-6.90	-13.00	2.30	1.45					
	Half	0.18	15	37	-3.60	-8.50	0.90	0.41	0.05	100	105	-4.90	-15.10	2.30	2.10					
	Double	0.70	15	37	0.70	-2.60	0.20	0.12	0.20	100	105	-5.90	-8.70	1.80	0.90					
	P and R	0.35	7.5	18.5	-3.50	-4.80	0.92	0.38	0.10	50	52.5	-7.00	-12.90	2.05	1.45					
	Double	0.35	30	74	4.92	-5.20	0.46	0.36	0.10	200	210	-6.90	-13.20	2.43	1.45					
	P or R	0.35	15	18.5	-4.20	-4.70	0.80	0.26	0.10	100	52.5	-6.80	-11.60	1.26	1.01					
	R half	0.35	7.5	37	2.90	-5.10	0.66	0.52	0.10	50	105	1.90	-17.10	2.60	3.03					
	P or R	0.35	15	74	13.30	-5.70	-0.14	0.50	0.10	100	210	21.50	-23.70	2.03	3.29					
	R double	0.35	30	37	-3.90	-4.80	1.08	0.26	0.10	200	105	-6.40	-13.10	2.02	0.96					

creased  $N_2$  concentration, were higher during the day and low (or below the detection limit) at night (Fig. 1). Although net daytime  $O_2$  production was not observed during summer (August), a diel pattern in  $N_2$  production (i.e., higher during the day than at night, Fig. 1; Table 5) was still evident. This pattern suggests that benthic primary production stimulated denitrification in this system. For benthic primary production to be important, benthic microphytes must be present, and they must have access to required nutrients and energy (i.e., sufficient PAR must reach the bottom).

Substantial Chl *a* was present in the sediments throughout Galveston Bay (250–800 mg Chl *a*  $m^{-2}$ ), whereas the phaeophytin concentration was negligible (An 1999). Pore-water nutrient concentrations exceeded those in the water column by a factor of 10 or more. Thus, on the basis of chlorophyll and nutrient data, these sediments are capable of supporting primary production. At the Texas City station, SCUBA divers were able to visualize the sediment-water interface inside the chambers when diving at high tide, illustrating that PAR reaches the bottom (S. An and S. Joye pers. observation). We estimated the sediment PAR flux from secchi depth data. The light attenuation coefficient ( $K_d$ ), as derived from the secchi depth data (secchi depth  $\sim 1.2$  and  $1.3$  m in January and August, respectively), ranged between  $0.99$  and  $1.4\ m^{-1}$  (January 1997) and  $0.92$  and  $1.3\ m^{-1}$  (August 1997). Under the assumption of a 4-m-deep water column (on average) and with use of the  $K_d$  values above, between 0.4% and 3% of surface PAR would reach the bottom. At a surface irradiance of 2000 (January) or 3000 (August)  $\mu E\ m^{-2}\ s^{-1}$ , the bottom PAR flux would have been between 7 and 38  $\mu E\ m^{-2}\ s^{-1}$  (January) or 17 and 76  $\mu E\ m^{-2}\ s^{-1}$  (August). This is ample energy to support substantial rates of benthic photosynthesis (Pinckney and Zingmark 1993).

*Height of boxes and maximum respiration and photosynthetic rates*—Since coupled denitrification occurs primarily in Box 2, the oxic-suboxic surface sediment, the height of this box is an important determinant for predicting rates and concentration changes. The factors controlling the  $O_2$  penetration depth include the rates of downward  $O_2$  diffusion,  $O_2$  consumption,  $O_2$  production by benthic microalgae (Revsbech et al. 1988), downward advection of  $O_2$  via bioirrigation (Aller 1980), and the sediment's permeability and porosity (Capone and Kiene 1988). The remineralization rate estimated from the DIC flux was four times greater during summer (An 1999). We surmised, therefore, that the  $O_2$  penetration depth would decrease during summer. We used the same height for Box 1 (1 cm) during both summer and winter; however, a shorter diffusion distance,  $X_i$ , was required in summer (0.1 cm), relative to winter (0.35 cm), to reproduce the observed  $O_2$  flux. We realize that higher rates of  $O_2$  uptake and DIC release could be supported by either steeper interfacial gradients (smaller  $X_i$  but no change in advection) or by elevated rates of bioirrigation relative to diffusive transport (same  $X_i$  but increased advection). Since the activity of benthic organisms increases during summer, enhanced bioirrigation could increase material exchange at the sediment water interface, contributing to the observed increase in remineralization rate (Aller 1980). Although both mechanisms are accounted for by changing the diffusive

Table 5. Values for the average (AVG) and standard deviation (STD) of  $N_2$  and  $O_2$  concentration during in situ sediment chamber incubations. The level of significance ( $P$ ) was derived using a one-tailed  $t$ -test. Significant ( $P < 0.05$ ) concentration changes are marked with an asterisk;  $n$  = number of individual gas samples used to determine the average.

Month	Sampling point ( $N$ )	Incubation time (h)	Dissolved nitrogen ( $N_2$ )				Dissolved oxygen ( $O_2$ )					
			AVG $N_2$ ( $\mu$ M)	STD	$n$	Significance level ( $P$ value)		AVG $O_2$ ( $\mu$ M)	STD	$n$	Significance level ( $P$ value)	
						Time $N + 1$ vs. time $N$	Time 0 vs. time $N$				Time $N + 1$ vs. time $N$	Time 0 vs. time $N$
Jan 1997	0	0	487.2	1.3	5			259.6	1.9	5		
	1	20	489.9	1.8	6	0.06		195.2	2	6	0.001*	
	2	30	497.0	1.8	6	0.001*	0.002*	240.2	3.8	6	0.001*	0.001*
Aug 1997	0	0	446.1	3.7	8			222.8	1.4	8		
	1	10	451.5	1.1	8	0.033*		141.5	50.6	8	0.005*	
	2	24	450.9	6.1	8	0.406	0.08	102.7	6.6	8	0.06	
	3	35	475.6	8.4	9	0.001*	0.001*	78.1	4.9	9	0.001*	0.001*

path length, supporting increased remineralization via a shorter diffusive path length may not be mechanistically correct.

Estimation of the role of benthic primary production in this system by use of our model requires reasonable estimates of  $P_{\max}$ . We measured significant rates of net photosynthesis (i.e., net  $O_2$  production up to  $16 \text{ mmol } O_2 \text{ m}^{-2} \text{ d}^{-1}$ ; An 1999) and gross photosynthetic rates, determined by use of paired light-dark chambers, are between 19 and  $65 \text{ mmol } O_2 \text{ m}^{-2} \text{ d}^{-1}$  (Warnken 1998). High benthic Chl  $a$  concentration, combined with secchi depth and PAR data, suggest that benthic photosynthesis is important in this system. However, photosynthetic rates achieved under nonsaturating irradiance is  $<3\%$ – $25\%$  those achieved under saturating irradiances (Falkowski and Raven 1997). Therefore, the summertime  $P_{\max}$  does not reflect the average gross rate but rather the rate achieved under conditions of low water column turbidity.

Model results of sediment oxygen demand (SOD) and denitrification rates obtained using various  $X_i$ ,  $R_{O_{\max}}$ , and  $P_{\max}$  conditions are shown in Table 4. During winter, a notable feature is daytime  $O_2$  production ( $\sim O_2$  efflux). This feature was reproduced under double  $P_{\max}$  or half  $R_{O_{\max}}$  conditions. However, these simulations underpredicted denitrification rates because high  $O_2$  concentrations inhibited denitrification. Doubling  $X_i$  reduced the benthic  $O_2$  efflux and elevated pore-water  $O_2$  concentration, thereby inhibiting denitrification. In the complete model, which simulated in situ conditions, the net SOD was lower during the day than at night ( $1.0$  vs.  $4.7 \text{ mmol m}^{-2} \text{ d}^{-1}$ ), underscoring the importance of photosynthesis in the net benthic  $O_2$  budget (Table 4). During summer, the net SOD was similar during day and night, and neither the SOD nor the denitrification rate was sensitive to variations in both  $R_{O_{\max}}$  and  $P_{\max}$  (Table 4). Denitrification rates in half  $R_{O_{\max}}$  or double  $P_{\max}$  simulations were low because of  $O_2$  inhibition, similar to the winter results. Low denitrification rates under half  $P_{\max}$  conditions were probably the result of  $O_2$  limitation of nitrification rather than  $O_2$  inhibition of denitrification (Table 4).

*Comparison of modeled rates and fluxes to observed data*—The diel pattern of dissolved gas and DIN concentration documented during in situ chamber incubations and those obtained from model output are shown in Figs. 2 and 3 and Table 6. Note that concentration data for all parameters was available only for Box 1, but the range of pore-water DIN concentrations measured in sediment cores is presented as well (Figs. 2, 3g,h,k,l). The model reproduced the average winter and summer SOD (Table 6) and the measured  $O_2$  decrease over time during summer (Fig. 3a). Net daytime  $O_2$  production was not as evident in the model results, despite the fact that pore-water  $O_2$  concentrations in Box 2 increased during day (Figs. 2a,e, 3a,e).

Model-derived daily integrated fluxes of  $O_2$  and  $N_2$  agreed well with fluxes observed in chambers (Table 6). Denitrification rates obtained from C:N flux stoichiometry ([denitrification rate = (DIC flux  $\times$  N:C ratio of reacting sediment organic matter) – DIN flux]; Joye et al. 1996b) were comparable to observed and model-derived rates. The fact that all three methods generate comparable rates suggests that the model is accurately simulating in situ processes. However,

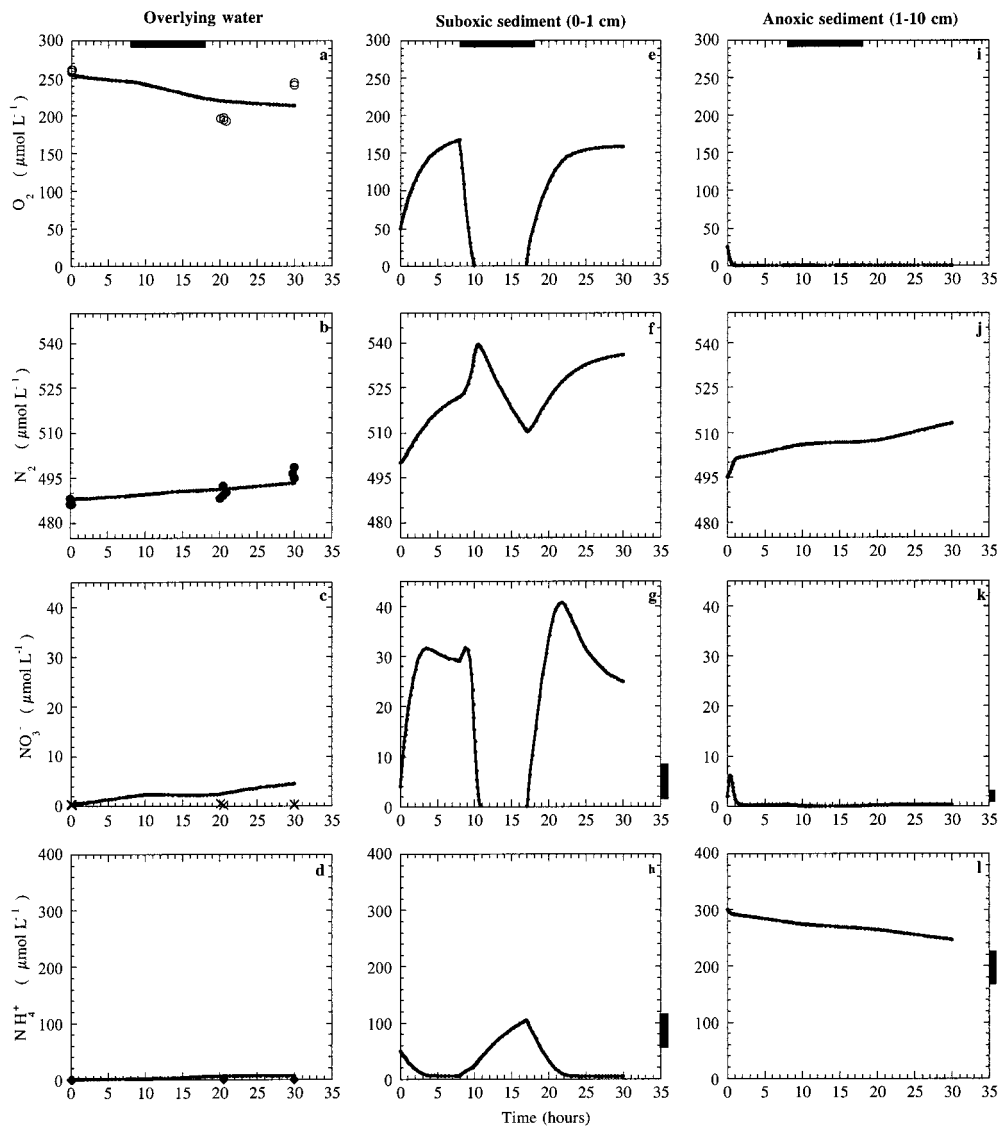


Fig. 2. Transient model results (line) and measured data (symbols) for Texas City incubations in January 1997. Concentration changes of  $N_2$ ,  $O_2$ ,  $NH_4^+$ , and  $NO_3^-$  were measured in the overlying water during the incubation. Each symbol represents data from three incubation chambers. Concentrations observed in the pore water (*g, h, k, l*) are shown by the bars to the right of the panels; these concentrations were measured only at time zero and the bar represents the average concentration for the depth interval (0–1 cm for suboxic sediments and 1–10 cm for anoxic sediments). The filled bar on the top *x* axis of panels *a, e, and i* represent the dark portion of the incubation.

the model overpredicted DIN fluxes during winter, and model-derived summer fluxes deviated from observed fluxes by a factor of two to four. Sediment water interface DIN fluxes were small, compared with rates of processes affecting DIN concentration (Figs. 2, 3*c,d*), suggesting that processes responsible for DIN consumption may be substrate limited (Henriksen and Kemp 1988; Koike and Sørensen 1988) and that DIN is efficiently cycled within the upper sediment layers, with negligible return to the water column as bioavailable inorganic N (Table 6). In fact, ~75% of the interfacial N flux is composed of dinitrogen. The low DIN fluxes observed in chambers could result from luxury DIN consumption by benthic microalgae (Joye et al. 1996*a*; Falkowski and Raven 1997). Alternatively, small deviations in the assumed C:N uptake ratio for benthic microalgae (~6.6 or the Red-

field ratio) could significantly alter model estimates of DIN consumption and impact model-derived DIN fluxes. In either case, the important point is that  $N_2$  was the primary inorganic N compound fluxing from sediments.

Diurnal variation in  $N_2$  concentrations, i.e., denitrification rates, was observed during in situ incubations (Fig. 1). In model simulations, day vs. night denitrification rates were estimated from the change in  $N_2$  concentration over time (Figs. 2, 3). Daytime rates were 1.4 and 3.7  $mmol\ m^{-2}\ d^{-1}$  in winter and summer, respectively, whereas nighttime rates were 0.10 and 0.24  $mmol\ m^{-2}\ d^{-1}$  in winter and summer, respectively (Figs. 2, 3*b*). Model-derived (24-h) denitrification rates were similar to the observed rates (Table 6). The temporal resolution of our chamber data did not permit us to evaluate rate variability at hourly timescales.

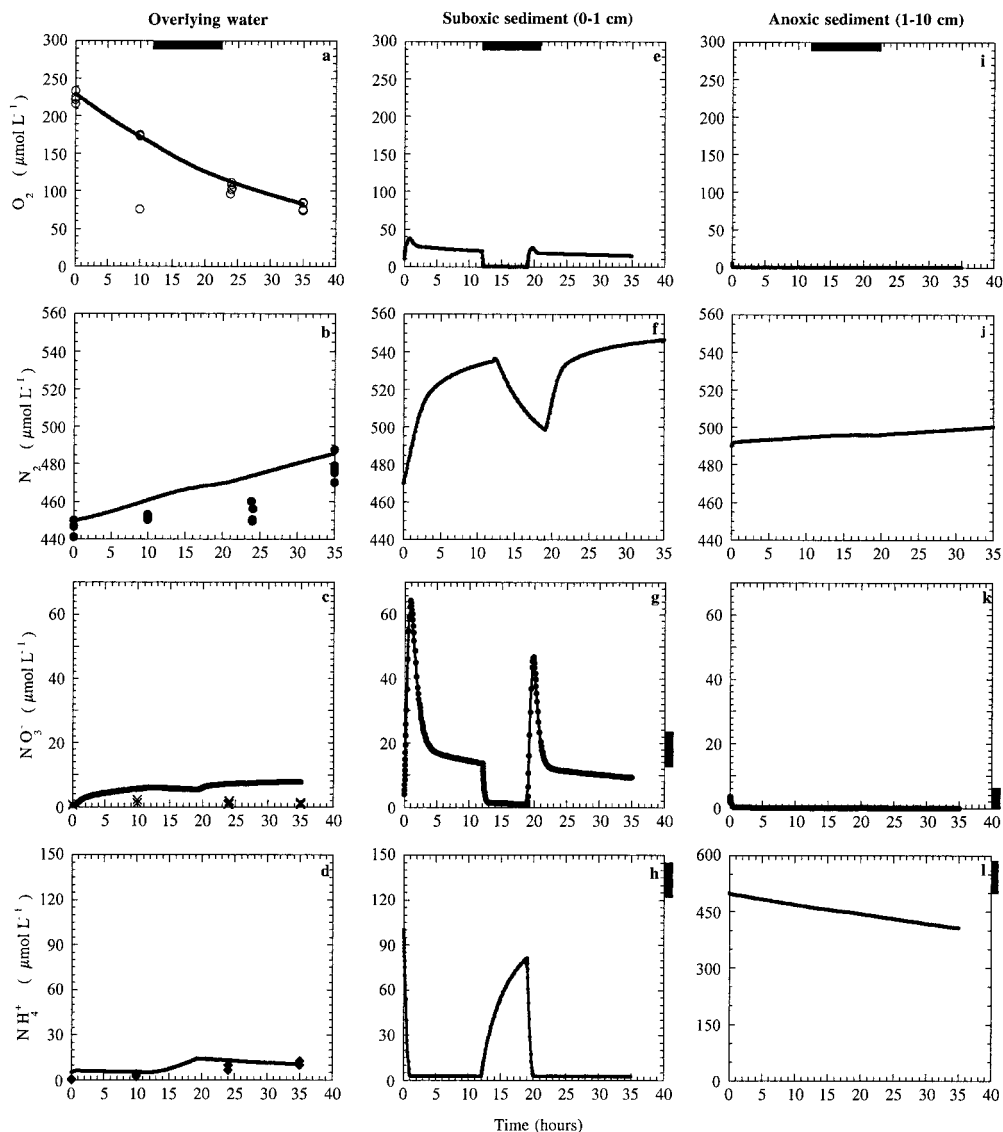


Fig. 3. Transient model results (line) and measured data (symbols) for Texas City incubations in August 1997. Concentration changes of  $N_2$ ,  $O_2$ ,  $NH_4^+$ , and  $NO_3^-$  were measured in the overlying water during the incubation. Each symbol represents data from three incubation chambers. Concentrations observed in the pore water (g, h, k, l) are shown by the bars to the right of the panels; these concentrations were measured only at time zero and the bar represents the average concentration for the depth interval (0–1 cm for suboxic sediments and 1–10 cm for anoxic sediments). The filled bar on the top x axis of panels a, e, and i represent the dark portion of the incubation.

However, we used the model output to explore the temporal evolution of  $O_2$  and  $N_2$  concentrations and to assess short-term interactions between denitrification and benthic photosynthesis. During winter, the variation of  $N_2$  concentration in Box 2 suggested that  $N_2$  concentration increased only during the first few hours of incubation. After that, no further increase was predicted, despite high  $NO_3^-$  concentrations (Figs. 2, 3f). These results suggest that high  $O_2$  concentration ( $>150 \mu M$ ) inhibited denitrification (Fig. 2e; Rysgaard et al. 1994). During summer, the  $NO_3^-$  concentration in Box 2 stabilized after 3 h (Fig. 3g), and the  $N_2$  concentration stabilized after 3 h (Fig. 3f). The pore-water  $O_2$  concentration in Box 2 did not exceed  $40 \mu M$ , and the inhibitory effect of  $O_2$  on denitrification was reduced. During summer, denitrification appeared to be limited by  $NO_3^-$  availability.

The dynamic variation in pore-water  $O_2$ ,  $N_2$ , and DIN concentrations predicted by the model suggest that the majority of denitrification activity occurs over short periods of time, in between which denitrification rates are low. When (benthic) primary production is important, denitrification rates probably fluctuate significantly, exhibiting morning and evening highs for example instead of constant activity over time. Similar patterns of diel variability in other  $O_2$ -sensitive N-cycling processes (i.e.,  $N_2$  fixation) have been documented in systems in which primary production is important (Bebout et al. 1987).

Exploring the model-derived temporal evolution of  $O_2$  and  $NH_4^+$  concentration provided insight to the factors influencing nitrification. Since nitrification and photosynthesis co-occur in Box 2, we focused on interactions between nitrification,

Table 6. Comparison of measured [average (SD)] and modeled daily (day plus night) sediment–water interface fluxes for summer and winter. For data derived from the transient model (“Model”), the flux represents exchange between Box 2 and Box 1 with positive denoting production and negative denoting consumption. Estimates of denitrification obtained from C:N flux stoichiometry (Stoich.) are presented for comparison. Fluxes are presented in  $\text{mmol m}^{-2} \text{d}^{-1}$ .

Variable	Winter			Summer		
	Observed	Model	Stoich.*	Observed	Model	Stoich.*
DIC	4.5 (0.2)	ND†	NA‡	18.76 (1.4)	ND	NA
O <sub>2</sub>	−1.8 (0.1)	−3	ND	−9.23 (0.7)	−11.90	ND
N <sub>2</sub>	0.58 (0.04)	0.50	0.68	1.93 (0.1)	2.30	1.84
NH <sub>4</sub>	0.00	0.50	ND	0.82 (0.1)	0.40	ND
NO <sub>3</sub>	−0.1 (0.02)	0.40	ND	0.2 (0.05)	0.80	ND

\* For the stoichiometric calculation, the observed (net) DIC flux was divided by the C:N ratio of reacting organic matter (6.6; see text for details) to estimate the net denitrification rate.

† ND = no data.

‡ NA = not applicable.

denitrification, and photosynthesis. The O<sub>2</sub> concentration in Box 2 reflects the balance between photosynthesis and O<sub>2</sub> consumption. During winter, O<sub>2</sub> concentration in Box 2 fluctuated between 0 and 185  $\mu\text{M}$  (Fig. 2e), and primary producers maintained low NH<sub>4</sub> concentration during the day. Low NH<sub>4</sub> concentration could limit nitrification (Fig. 2h); however, although modeled NH<sub>4</sub> concentrations were low, they did not reach zero, and daytime NO<sub>3</sub> accumulation suggested active nitrification. During the daytime in summer, NH<sub>4</sub> concentrations approached zero, O<sub>2</sub> concentrations were low, and NO<sub>3</sub> accumulation was reduced significantly (Fig. 3e,g,h). The low pore-water O<sub>2</sub> concentration permitted contemporaneous production (nitrification) and consumption (denitrification) of NO<sub>3</sub>, and this efficient coupling between the two processes prevented NO<sub>3</sub> accumulation during the day.

Model results suggest that when the N demand of benthic primary producers exceeds internal N regeneration, e.g., during winter, competition between nitrifiers and primary producers for NH<sub>4</sub> controls nitrification (Henriksen and Kemp 1988). During summer, however, N-regeneration rates increased and exceeded the N demand of benthic primary producers. At this time, restricted temporal overlap of NH<sub>4</sub> and O<sub>2</sub> availability probably controls nitrification (Fig. 4; Kemp et al. 1990). Although modeled concentrations of NO<sub>3</sub> and O<sub>2</sub> changed rapidly, the integrated denitrification rates were comparable to observed rates. Since O<sub>2</sub> and NO<sub>3</sub> concentration covary as a function of the O<sub>2</sub> dependence of nitrification, denitrification rates formed straight lines along the NO<sub>3</sub>–O<sub>2</sub> concentration plots (Fig. 4b,d). During winter, denitrification rates exhibited low variability, despite large fluctuations in O<sub>2</sub> concentration. Although photosynthetically driven increases in O<sub>2</sub> concentration stimulated nitrification, denitrification was inhibited by high O<sub>2</sub> concentration. Therefore, potential rates of coupled denitrification rates were limited during winter periods characterized by high photosynthetic rates and low respiration rates (Henriksen and Kemp 1988). In contrast, during summer, high daytime respiration maintained low O<sub>2</sub> concentrations in Box 2 (Fig. 3e), and this, combined with increased NO<sub>3</sub> availability, stimulated denitrification (Fig. 3e). When the pore-water O<sub>2</sub> concentration did not inhibit denitrification, benthic photosyn-

thesis stimulated rates of coupled denitrification (Risgaard-Petersen et al. 1994).

*Simulations under different O<sub>2</sub> and primary production conditions*—To further evaluate the impact of benthic primary production on N dynamics, two additional simulations were performed. Benthic photosynthesis was either prevented (“no photosynthesis”) or the O<sub>2</sub> concentration in Box 1 was held constant (“constant O<sub>2</sub>”). Calculated rates of net respiration, nitrification, and denitrification for each set of model conditions, “complete,” “constant O<sub>2</sub>,” and “no photosynthesis,” are shown in Table 7. These results illustrate convincingly that in the absence of benthic photosynthesis, O<sub>2</sub> concentration in Box 2 decreased to zero within 1 h, and sediments remained anoxic throughout the simulation, leading to NH<sub>4</sub> accumulation (Table 7). Reduced rates of respiration, nitrification, and denitrification were generated under no photosynthesis conditions (Table 7). Differences in rates between complete and constant O<sub>2</sub> simulations were large at night when the only O<sub>2</sub> source was diffusion from Box 1. Under constant O<sub>2</sub> conditions, high O<sub>2</sub> concentrations in Box 1 increased the O<sub>2</sub> gradient between Boxes 1 and 2, increasing the supply of O<sub>2</sub> to Box 2 and stimulating rates of respiration and nitrification (by 8%–40%; Table 7). Rates during the day were similar between complete and constant O<sub>2</sub> conditions.

The presence of an O<sub>2</sub> source was required to simulate the diel patterns we observed during chamber incubations. At the Texas City site, benthic photosynthesis provided most of the O<sub>2</sub> consumed during benthic metabolism. Benthic primary production also recaptured inorganic nutrients that would have otherwise been lost from the sediment compartment. Field and model results suggest that benthic primary production enhanced coupled denitrification in Galveston Bay sediments. The effects of benthic primary production on N cycling have not been extensively reported, primarily because of methodological problems that have led to the examination of N cycling under dark, rather than light, conditions. Perhaps the justification for this approach was that benthic photosynthesis in estuaries is unlikely, considering the turbid nature of these systems. Our data show clearly that this assumption is erroneous: a benthic primary

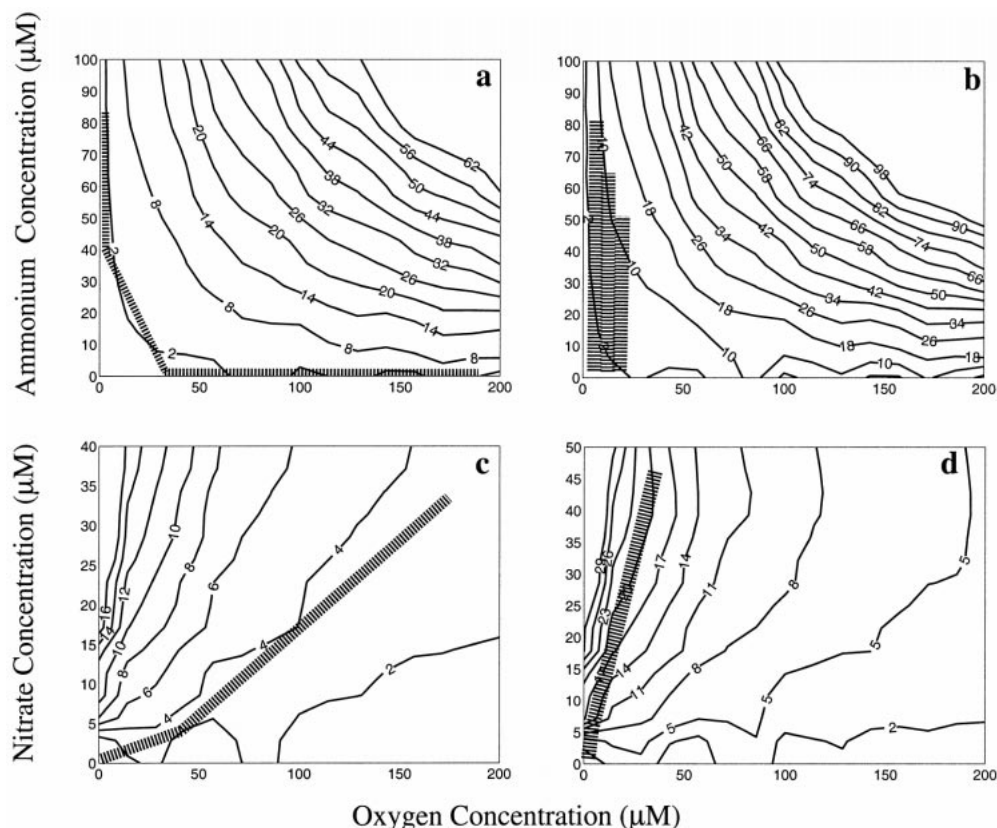


Fig. 4. (a, b) Model-derived nitrification and (c, d) denitrification rates under various  $\text{NH}_4$ ,  $\text{NO}_3$ , and  $\text{O}_2$  conditions. Winter rates are shown in panels a and c, whereas summer rates are shown in panels b and d. The hatched area depicts the range used for model runs.

production term was required to simulate N dynamics in Galveston Bay sediments.

Since benthic production is likely in other coastal systems (Mehercordt and Meyer-Reil 1999), the interactions between benthic primary production and N cycling that we have documented in Galveston Bay could be common in shallow coastal systems. If so, denitrification rates in shallow estuaries may have been underestimated in previous studies. Our estimates of N removal via denitrification are four times larger than those of Zimmerman and Benner (1994), who determined rates during dark incubations.

Furthermore, N loss via denitrification in this system exceeds that predicted by the hydraulic residence time–deni-

trification relationship (Nixon et al. 1996). On the basis of the hydraulic residence time in Galveston Bay (~40–50 d), N loss by denitrification should approach 35% of the N load to the system (Nixon et al. 1996). However, our data suggest that >50% of the N load was denitrified (An 1999). The enhancement of coupled denitrification by benthic photosynthesis results in elevated rates of N loss in this system and perhaps in coastal systems generally.

### References

ALLER, R. C. 1980. Relationships of tube-dwelling benthos with sediment and overlying water chemistry, p. 285–310. *In* K. R.

Table 7. Model estimates of the impact of benthic photosynthesis on respiration, nitrification, and denitrification rates. Results from the complete model, “constant  $\text{O}_2$ ” and “no benthic photosynthesis” schemes are presented as integrated rates for Boxes 2 and 3; units are  $\text{mmol m}^{-2} \text{d}^{-1}$ . For the constant  $\text{O}_2$  case, the  $\text{O}_2$  concentration in Box 1 was held constant.

	Model type	Winter			Summer		
		Complete	Constant $[\text{O}_2]$	No benthic photosynthesis	Complete	Constant $[\text{O}_2]$	No benthic photosynthesis
Respiration	Light	14.70	13.92	0.07	70.46	68.31	10.99
	Dark	1.09	8.54	1.66	5.54	16.07	4.78
Nitrification	Light	3.80	3.25	0.02	12.85	12.74	1.36
	Dark	0.13	2.08	0.33	0.45	1.51	0.52
Denitrification	Light	5.88	4.94	0.04	11.60	12.20	1.82
	Dark	0.64	3.50	0.74	1.53	1.93	0.56

- Tenore and B. C. Coull [eds.]. Marine benthic dynamics. Univ. of South Carolina Press.
- AN, S. 1999. Nitrogen cycling and denitrification in Galveston Bay. Ph.D. dissertation. Texas A&M University.
- , AND S. B. JOYE. 1997. An improved gas chromatographic method for measuring nitrogen, oxygen, argon and methane in gas or liquid samples. *Mar. Chem.* **59**: 63–70.
- BEBOUT, B. M., H. W. PAERL, K. M. CROCKER, AND L. E. PRUFERT. 1987. Diel interactions of oxygenic photosynthesis and nitrogen fixation ( $C_2H_2$  reduction) in a marine microbial mat community. *Appl. Environ. Microbiol.* **53**: 2353–2362.
- BOUDREAU, B. P. 1996. A method of line code for carbon and nutrient diagenesis in aquatic sediments. *Comp. Geosci.* **22**: 479–496.
- . 1997. Diagenetic models and their implementation. Springer Verlag.
- CAPONE, D. G., AND R. P. KIENE. 1988. Comparison of microbial dynamics in marine and freshwater sediments: Contrast in anaerobic carbon metabolism. *Limnol. Oceanogr.* **33**: 725–749.
- CHRISTENSEN, P. B., L. P. NIELSEN, N. P. REVSBECH, AND J. SØRENSEN. 1989. Microzonation of denitrification activity in stream sediments as studied with a combined oxygen and nitrous oxide microsensor. *Appl. Environ. Microbiol.* **55**: 1234–1241.
- DUCKLOW, H. W. 1983. Production and fate of bacteria in the oceans. *BioScience* **33**: 494–501.
- FALKOWSKI, P. G., AND J. A. RAVEN. 1997. Aquatic photosynthesis. Blackwell Science.
- GUERRERO, M. A., AND R. D. JONES. 1996a. Photoinhibition of marine nitrifying bacteria: I. Wavelength-dependent response. *Mar. Ecol. Prog. Ser.* **141**: 183–192.
- , AND ———. 1996b. Photoinhibition of marine nitrifying bacteria: II. Dark recovery after monochromatic or polychromatic irradiation. *Mar. Ecol. Prog. Ser.* **141**: 193–198.
- HENRIKSEN, K., J. I. HANSEN, AND T. H. BLACKBURN. 1981. Rates of nitrification, distribution of nitrifying bacteria, and nitrate fluxes in different types of sediment from Danish waters. *Mar. Biol.* **61**: 299–304.
- , AND W. M. KEMP. 1988. Nitrification in estuarine and coastal marine sediments: Methods, patterns and regulating factors, p. 207–250. *In* T. H. Blackburn and J. Sørensen [eds.], Nitrogen cycling in coastal marine environments. Wiley.
- HOWARTH, R. W., AND J. M. TEAL. 1979. Sulfate reduction in a New England salt marsh. *Limnol. Oceanogr.* **24**: 999–1013.
- , R. MARINO, AND J. LANE. 1988. Nitrogen fixation in freshwater and marine ecosystems. I. Rates and importance. *Limnol. Oceanogr.* **33**: 669–687.
- HOWES, B. L., J. W. H. DACEY, AND G. M. KING. 1984. Carbon flow through oxygen and sulfate reduction pathways in salt marsh sediments. *Limnol. Oceanogr.* **29**: 1037–1051.
- JØRGENSEN, B. B. 1977. The sulfur cycle of coastal marine sediment (Limfjorden, Denmark). *Limnol. Oceanogr.* **22**: 814–832.
- JOYE, S. B., AND J. T. HOLLIBAUGH. 1995. Sulfide inhibition of nitrification influences nitrogen regeneration in sediments. *Science* **270**: 623–625.
- , M. L. MAZZOTTA, AND J. T. HOLLIBAUGH. 1996a. Community metabolism in intertidal microbial mats: the importance of iron and manganese reduction. *Estuar. Coast. Shelf Sci.* **43**: 747–766.
- , L. G. MILLER, T. L. CONNELL, R. JELLISON, AND R. S. OREMLAND. 1999. Oxidation of methane and ammonia in an alkaline, saline lake. *Limnol. Oceanogr.* **44**: 178–188.
- , S. V. SMITH, J. T. HOLLIBAUGH, AND H. W. PAERL. 1996b. Estimating denitrification in estuarine sediments: Comparisons of stoichiometric and acetylene based methods. *Biogeochemistry (Dordr.)* **33**: 197–215.
- KEMP, W. M., P. SAMPOU, AND M. MAYER. 1990. Ammonium recycling versus denitrification in Chesapeake Bay sediment. *Limnol. Oceanogr.* **35**: 1545–1563.
- KOIKE, I., AND J. SØRENSEN. 1988. Nitrate reduction and denitrification in marine sediments, p. 251–274. *In* T. H. Blackburn and J. Sørensen [eds.]. Nitrogen cycling in coastal marine environments. Wiley.
- KOROLEFF, F., AND K. GRASSHOFF. 1983. Determination of nutrients, p. 125–188. *In* K. Grasshoff, M. Ehrhardt and K. Kremling [eds.]. Methods of seawater analysis. Weinheim Verlag Chemie Publ.
- MEHERCORDT, J., AND L.-A. MEYER-REIL. 1999. Primary production of benthic microalgae in two shallow coastal lagoons of different trophic status in the southern Baltic Sea. *Mar. Ecol. Prog. Ser.* **178**: 179–191.
- MIDDELBURG, J. J., K. SOETAERT, S. M. J. HERMAN, AND C. H. R. HEIP. 1996. Denitrification in marine sediment: A model study. *Global Biogeochem. Cycles* **10**: 661–673.
- NIELSEN, L. P., P. B. CHRISTENSEN, N. P. REVSBECH, AND J. SØRENSEN. 1990. Denitrification and photosynthesis in stream sediment studied with microsensor and whole-core techniques. *Limnol. Oceanogr.* **35**: 1135–1144.
- , AND N. P. SLOTH. 1994. Denitrification, nitrification and nitrogen assimilation in photosynthetic microbial mats, p. 319–324. *In* L. J. Stahl and P. Caumette [eds.]. Microbial mats: structure, development and ecological significance. NATO ASI, series G, ecological sciences, v. 35. Springer-Verlag.
- NIXON S. W., AND OTHERS. 1996. The fate of nitrogen and phosphorus at the land-sea margin of the North Atlantic Ocean, p. 25–47. *In* R. Howarth [ed.]. Nitrogen cycling in the North Atlantic Ocean and its watershed. Kluwer.
- PINCKNEY, J. L., R. PAPA, AND R. ZINGMARK. 1994. Comparison of high-performance liquid chromatography, spectrophotometric and fluorometric methods for determining chlorophyll *a* in estuarine sediments. *J. Microbiol. Methods* **19**: 59–66.
- , AND R. G. ZINGMARK. 1993. Modeling the annual production of intertidal benthic microalgae in estuarine ecosystems. *J. Phycol.* **29**: 396–407.
- REVSBECH, N. P., J. NIELSEN, AND P. K. HANSEN. 1988. Benthic primary production and oxygen profile, p. 69–84. *In* T. H. Blackburn and J. Sørensen [eds.]. Nitrogen cycling in coastal marine environments. Wiley.
- RISGAARD-PETERSON, N., S. RYSGAARD, L. P. NIELSEN, AND N. P. REVSBECH. 1994. Diurnal variation of denitrification and nitrification in sediments colonized by benthic microphytes. *Limnol. Oceanogr.* **39**: 573–579.
- RYSGAARD, S., P. B. CHRISTENSEN, AND L. P. NIELSEN. 1995. Seasonal variation in nitrification and denitrification in estuarine sediment colonized by benthic microalgae and bioturbating infauna. *Mar. Ecol. Prog. Ser.* **126**: 111–121.
- SEITZINGER, S. P. 1990. Denitrification in aquatic sediments, p. 301–322. *In* N. P. Revsbech and J. Sørensen [eds.]. Denitrification in soil and sediment. Plenum.
- SOLARANZO, L. 1969. Determination of ammonia in natural waters by the phenol hypochlorite method. *Limnol. Oceanogr.* **14**: 799–801.
- SØRENSEN, J., B. B. JØRGENSEN, AND N. P. REVSBECH. 1979. A comparison of oxygen, nitrate and sulfate respiration in coastal marine sediments. *Microb. Ecol.* **5**: 105–115.
- TIEDJE, J. M., S. SIMKINS, AND P. M. GROFFMAN. 1989. Perspectives on measurement of denitrification in the field including recommended protocols for acetylene-based methods. *Plant Soil* **115**: 261–284.
- TOMASZEK, J. A., W. S. GARDNER, AND T. H. JOHENSEN. 1997. Denitrification in sediments of Lake Erie coastal wetland (Old

- Woman Creek, Huron, Ohio, USA). *J. Gt. Lakes Res.* **23**: 403–415.
- VAN CAPPELLEN, P., AND Y. WANG. 1996. Cycling of iron and manganese in the surface sediments: A general theory for the coupled transport and reaction of carbon, oxygen, nitrogen, sulfur, iron, and manganese. *Am. J. Sci.* **296**: 197–243.
- WANG, Y., AND P. VAN CAPPELLEN. 1996. A multicomponent reactive transport model of early diagenesis: Application to redox cycling in coastal marine sediments. *Geochim. Cosmochim. Acta* **60**: 2993–3014.
- WARD, B. B., K. A. KILPATRICK, E. RENGER, AND R. W. EPPLEY. 1989. Biological nitrogen cycling in the nitracline. *Limnol. Oceanogr.* **34**: 493–513.
- WARNKEN, K. W. 1998. Sediment water exchange of trace metals and nutrients in Galveston Bay, Texas. M.S. thesis. Texas A&M University.
- ZIMMERMAN, A. R., AND R. BENNER. 1994. Denitrification, nutrient regeneration and carbon mineralization in sediments of Galveston Bay, Texas, USA. *Mar. Ecol. Prog. Ser.* **114**: 275–288.

*Received: 29 October 1999*

*Accepted: 10 July 2000*

*Amended: 19 September 2000*